periodica polytechnica

Civil Engineering
58/2 (2014) 155–171
doi: 10.3311/PPci.7550
http://periodicapolytechnica.org/ci

RESEARCH ARTICLE

An efficient hybrid particle swarm strategy, ray optimizer, and harmony search algorithm for optimal design of truss structures

Ali Kaveh / *Seyed Mohammad* Javadi
Received 2013-12-12, accepted 2014-03-10

Abstract

In this paper a metaheuristic algorithm composed of particle swarm, ray optimization, and harmony search (HRPSO) is presented for optimal design of truss structures. This algorithm is based on the particle swarm ray origin making is used to update the positions of the particles, and for enhancing the exploitation of the algorithm the harmony search is utilized. Numerical results demonstrate the efficiency and robustness of the HRPSO method compared to some standard metaheuristic algorithms.

Keywords

Particle swarm optimization · Ray optimization · Harmony search · Truss structures design · Size optimization

Ali Kaveh

Centre of Excellence for Fundamental Studies in Structural Engineering, School of Civil Engineering, Iran University of Science and Technology, Tehan-16, Iran
e-mail: alikaveh@iust.ac.ir

Seyed Mohammad Javadi

Centre of Excellence for Fundamental Studies in Structural Engineering, School of Civil Engineering, Iran University of Science and Technology, Tehan-16, Iran

1 Introduction

Metaheuristic algorithms have become powerful tools for optimizing many problems in different fields of engineering. Examples of such algorithms are GA algorithm [1], Particle Swarm Optimization algorithm [2, 3], Ant Colony Optimization algorithm [4], Charged System Search [5] Ray Optimization [6] and many other algorithms. Apart from these basic algorithms, researchers are still striving to balance the exploration and exploitation abilities of the metaheuristic algorithms, Some examples of these are a hybrid PSO with the passive congregation (PSOPC) [7], a hybrid PSO with ACO and HS utilized for controlling the variable constraint (HPSACO) [8], a hybrid method ANGEL, which combined ant colony optimization (ACO), genetic algorithm (GA), and local search strategy (LS) [9, 10], among others

Recently, structural optimization has become one of the most popular fields of optimization science. Different algorithms have been employed for structural optimization including Genetic Algorithms [11], Ant Colony Optimization [12], Particle Swarm Optimizer [13,14], Harmony Search [15], Big Bang–Big Crunch [16] Structural optimization has been studied in three major groups as: (a) Size optimization (b) Topology optimization (c) Shape optimization.

In this paper, the mixed particle swarm ray optimization and harmony search is applied to the size optimization of truss structures. In this algorithm, PSO acts as the main engine of the algorithm, RO boost the movement vector of the particles and HS enhances the local search for better exploitation.

2 A brief introduction to the PSO, HS and RO

2.1 Particle swarm optimization

Particle swarm optimization (PSO) is a simple and effective algorithm for optimizing a wide range of functions. Conceptually, it seems to lie somewhere between genetic algorithm and evolutionary programming [2] The PSO uses the real-number randomness and the global communication among the swarm particles. In this sense, it is also easier to implement as there is no encoding or decoding of the parameters into binary strings as in genetic algorithms [17]. On each iteration, the swarm is updated by the following equations [3, 18]:

$$V_i^{k+1} = \omega V_i^k + c_1 r_1 \left(P_i^k - X_i^k\right) + c_2 r_2 \left(P_g^k - X_i^k\right) \quad (1)$$

$$X_i^{k+1} = X_i^k + V_i^{k+1} \quad (2)$$

where P_i is the best previous position of the ith particle and P_g is the best position of the particles which ever found. ω is an inertia weight to control the influence of the previous velocity, c_1 and c_2 are two acceleration constants and r_1 and r_2 are two random numbers uniformly distributed in the range of (0,1). The flowchart of the PSO is shown in Fig. 1.

2.2 Harmony search

The Harmony search algorithm was conceptualized using the musical process of searching for a perfect state of harmony. Musical performances seek to find pleasing harmony as determined by an aesthetic standard, just as the optimization process seeks to find a global solution as determined by an objective function. The pitch of each musical instrument determines the aesthetic quality [19].

Fig. 2 shows the optimization procedure of the HS algorithm, which consists of the following steps [15]:

Step 1: Initialize the optimization problem and the algorithm parameters such as specification of each decision variable, possible value range for each decision variable, harmony memory size (HMS), harmony memory considering rate (HMCR), pitch adjusting rate (PAR), harmony memory (HM) and termination criterion.

Step 2: Improvise a new harmony from the HM. A new harmony vector is generated from the HM based on memory considerations rate (HMCR), pitch adjustments and randomization (PAR). The HMCR sets the rate of choosing one value from the historic values stored in the HM, and (1−HMCR) sets the rate of randomly choosing one value from the possible range of values. While the HMCR varies between 0 and 1, the pitch adjusting process is performed only after a value is chosen from the HM. The value (1−PAR) sets the rate of doing nothing. If the pitch adjustment decision for x_i is yes then

$$x_i' \leftarrow x_i' + bw.u(-1, 1)$$

where bw is an arbitrary distance bandwidth for the continuous design variable and $u(-1, 1)$ is a uniform distribution between −1 and 1 The HMCR and PAR parameters introduced in the harmony search help the algorithm to find globally and locally improved solutions, respectively [19].

Step 3: Update the HM. In Step 4, if the New Harmony is better than the worst harmony in the HM, the New Harmony is included in the HM and the existing worst harmony is excluded from the HM. The HM is then sorted by the value of the objective function.

Step 4: Repeat Steps 2 and 3 until the termination criterion is satisfied. The computations are terminated when the termination criterion is satisfied. Otherwise, steps 2 and 3 are repeated.

2.3 Ray optimization

Ray optimization (RO) is recently developed by Kaveh and Khayatazad [6] This method is inspired by the transition of ray from one medium to another from physics and uses the Snell's refraction law of the light. The transition of the ray is utilized for finding the global or near-global solution.

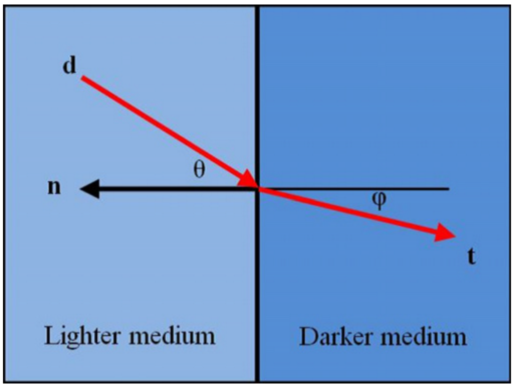

Fig. 3. Incident and refracted rays and their specifications.

The pseudo-code of RO is presented in the following [20]:

Level 1: Scattering and evaluation

Step 1. Initialization. Initialize the parameter of the RO. Initialize an array of agents with random positions. According to the number and type of groups that belong to the agent positions, make an arbitrary array of the velocity vector. Each of these two or three variable velocity vectors should be a normalized vector.

Step 2. Evaluation. For each agent evaluate the value of the goal function in the current position. Save the position of the best agent as the global best. Save the position of each agent as its local best.

Level 2: Movement vector and motion refinement

Step 1. Movement vector. Add the solution vectors with the corresponding movement vector.

Step 2. Motion refinement. If any agent violates a variable boundary, refine its movement vector. After motion refinement and evaluation of the goal function, again the so-far best agent at this stage is selected as the global best, and for each agent, the so-far best position by this stage (belonging to itself) is selected as its local best.

Level 3: Origin making and converging

Step 1. Origin making. Find the origin of the each agent.

Step 2. Converging. Calculate the new movement vector for each agent.

Level 4: Finish or redoing. Repeat the optimization process until a terminating criteria is satisfied.

3 Mixed particle swarm, ray optimization, and harmony search algorithm

Compared to other algorithms, PSO has a versatility to be hybridized with other metaheuristics and simple to implement. However, standard PSO has some infirmity, Shi and Eberhart [18] introduced a parameter known as the inertia weight into

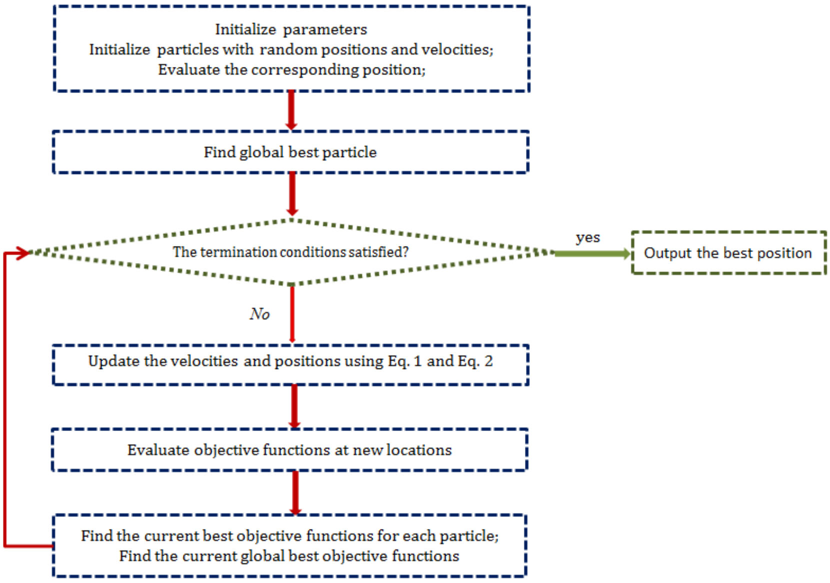

Fig. 1. Flowchart of the PSO.

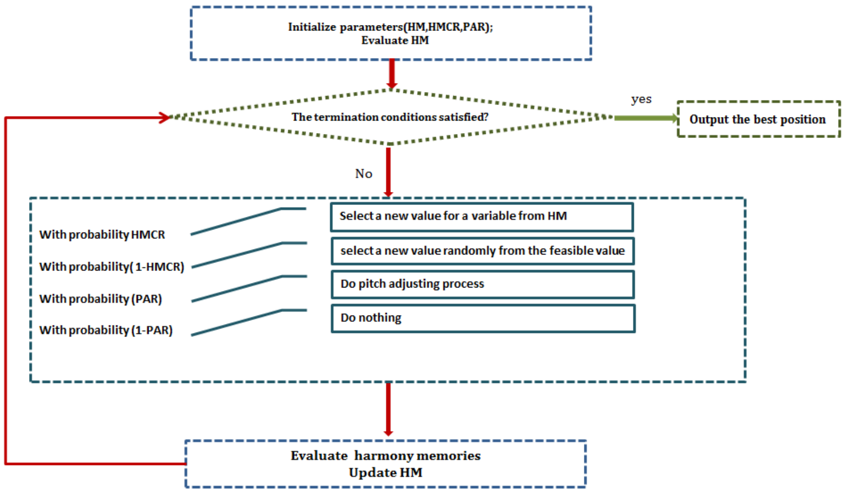

Fig. 2. Flowchart of the HS.

the original particle swarm optimizer, to decrease the computational time and improve ability in finding the global optimum. However, there is no information sharing among individuals except that *global best* broadcasts the information to the other individuals. Therefore, the population may lose diversity and is more likely to confine the search around local minima if committed too early in the search to the global best found so far He et al. [7] introduced a new PSO with the passive congregation (PSOPC), by introducing the passive congregation, information can be transferred among individuals that will help individuals to avoid misjudging information and becoming trapped by poor local minima. Therefore in the PSOPC there are parameters such as c_1, c_2 and c_3 with each of them having an important role on the performance of the algorithm.

On the other hand Ray optimization algorithm has an origin making part which has an important role in this algorithm. In the RO first the point to which each particle moves must be determined. This point is named origin and it is specified by:

$$O_i^k = \frac{(ite + k).GB + (ite - k).LB_i}{2.ite} \tag{3}$$

Where O_i^k is the origin of the ith agent or particle for the kth iteration, *ite* is the total number of iterations of the optimization process, GB and LB_i are the global best and local best of the ith agent, respectively [6]. In HRPSO ray origin making is used to update the positions of the particles by the following equations:

$$V_i^{k+1} = \omega V_i^k + rand.O_i^k \tag{4}$$

Thus in this algorithm. Parameters such as c_1, c_2 and $c_3$in standard PSO and PSO with the passive congregation (PSOPC) substitute with origin making relation which is independent from parameter tuning. In this equation the inertia weight considered as a decreasing function of time which gradually decrease from 1 by each iteration and *rand* is a random number between 0 and 1.

On the other hand for enhancing the exploitation, the HS introduces a parameter named pitch adjustment which helps the algorithm find locally improved solutions [19] so the PAR used to reinforce the HRPSO for better local search.

By these techniques, there is no dependency on the parameters like as c_1, c_2 and c_3 in the PSO and PSOPC. The flow chart of the HRPSO is shown in Fig. 4.

4 STRUCTURAL OPTIMIZATION PROBLEM

The mathematical formulation of this optimization problem can be expressed as:

$$\begin{aligned}
&\text{minimize} W(\{X\}) = \sum_{i=1}^{n} \gamma_i A_i L_i(x) \\
&\text{subject to : } \delta_{min} \le \delta_i \le \delta_{max}, i = 1, 2, ..., m \\
&\sigma_{min} \le \sigma_i \le \sigma_{max}, i = 1, 2, ..., n \\
&\sigma_i^b \le \sigma_i \le 0, i = 1, 2, ..., ns \\
&A_{min} \le A_i \le A_{max}, i = 1, 2, ..., ng
\end{aligned}$$

Where $W(\{X\})$ is the weight of the structure; m is the number of nodes; n is the number of members making up the structure; ns is the number of compression elements; ng is the number groups (number of design variables); γ_i is the material density of member i; L_i is the length of member i; A_i is the cross-sectional area of member i chosen between A_{min} and A_{max}; min is the lower bound and max is the upper bound; σ_i and δ_i are the stress and nodal deflection, respectively; σ_i^b is the allowable buckling stress in member i when it is in compression.

The penalty approach is used for constraint handling, i.e., if the constraints are not violated, the penalty will be zero; otherwise, the value of the penalty is calculated by dividing the violation of the allowable limit to the limit itself.

5 DESIGN EXAMPLES

In this section, four truss structures are optimized utilizing the present algorithm. These optimization examples consist of a 25 bar space truss subjected to two load conditions, a 72 bar space truss subjected to two load conditions, a 120 bar dome space truss subjected to a single load condition and a 200 bar planar truss subjected to three load conditions.

In the proposed algorithm, the maximum number of iterations is set equal to 400, a population of 40 particles is used for the first example, a population of 60 particles is utilized for the second example and a population of 90 particles is employed for two last examples. The maximum velocity is set as the difference between the upper and lower bounds, which guarantees that the particles rationally survey the search space and pitch adjusting rate (PAR) consider as 0.2. These truss structures are analyzed using the finite element method (FEM).

5.1 A 25-bar space truss

The topology and nodal numbers of a 25-bar spatial truss structure are shown in Fig. 5. This structure has been size optimized by many researchers and the results are compared. In these studies, the material density was 0.1 lb/in^3 (2767.990 kg/m^3) and modulus of elasticity was 10,000 ksi (68950 MPa), Twenty five members are categorized into eight groups, as shown in Tab. 1. Designs for a multiple load case are performed as shown in Tab. 2. The truss members are subjected to the compressive and tensile stress limitations shown in Tab. 3.

In addition, maximum displacement limitations of ± 0.35 in (8.89 mm) are imposed on every node in every direction. The

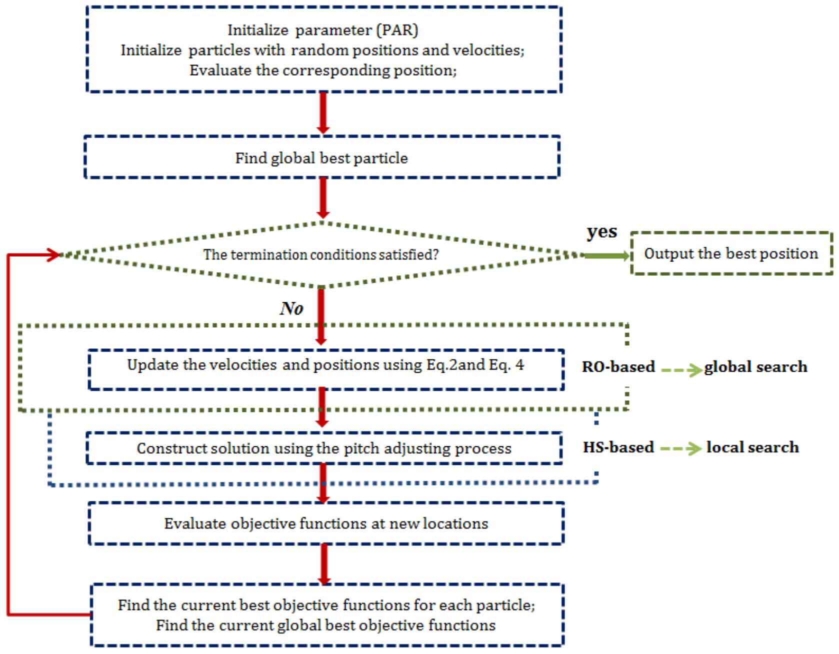

Fig. 4. Flowchart of the HRPSO.

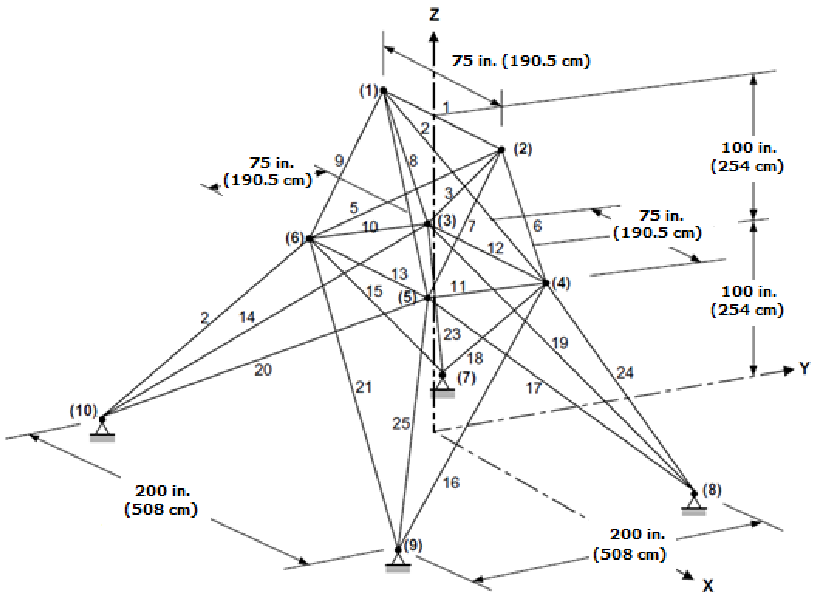

Fig. 5. A 25-bar spatial truss.

Tab. 1. Element information for the 25-bar spatial truss.

Element group number							
1	2	3	4	5	6	7	8
1;(1,2)	2:(1,4)	6:(2,4)	10:(6,3)	12:(3,4)	14:(3,10)	18:(4,7)	22:(10,6)
	3:(2,3)	7:(2,5)	11:(5,4)	13:(6,5)	15:(6,7)	19:(3,8)	23:(3,7)
	4:(1,5)	8:(1,3)			16:(4,9)	20:(5,10)	24:(4,8)
	5:(2,6)	9:(1,6)			17:(5,8)	21:(6,9)	25:(5,9)

Tab. 2. Loading conditions for the 25-bar spatial truss.

Node	Case1			Case2		
	P_X	P_Y kips (kN)	P_Z kips(kN)	P_X kips (kN)	P_Y kips (kN)	P_Z kips (kN)
1	0.0	20.0 (89)	-5.0 (22.25)	1.0 (4.45)	10 (44.5)	-5.0 (22.25)
2	0.0	-20.0 (89)	-5.0 (22.25)	0.0	10 (44.5)	-5.0 (22.25)
3	0.0	0.0	0.0	0.5 (2.22)	0.0	0.0
6	0.0	0.0	0.0	0.5 (2.22)	0.0	0.0

Tab. 3. Member stress limitation for the 25-bar spatial truss.

	Element group	Compressive stress limitations ksi (MPA)	Tensile stress limitations Ksi
1	A1	35.092 (241.96)	40.0 (275.80)
2	A2~A5	11.590 (79.913)	40.0 (275.80)
3	A6~A9	17.305 (119.31)	40.0 (275.80)
4	A10~A11	35.092 (241.96)	40.0 (275.80)
5	A12~A13	35.092 (241.96)	40.0 (275.80)
6	A14~A17	6.759 (46.603)	40.0 (275.80)
7	A18~A21	6.959 (47.982)	40.0 (275.80)
8	A22~A25	11.082 (76.410)	40.0 (275.80)

minimum and maximum cross-sectional area of all members is 0.01 in^2 (0.06452 cm^2) and 3.4 in^2 (21.94 cm^2) respectively A comparison to other references with respect to the cross-sectional area of each group and the final weight reached for the 25 bar space truss is shown in the Tab. 4. Fig. 6 and Fig. 7 compare the allowable existing stress and displacement constraint values of the HRPSO resulted for two different loading conditions. The comparison of the results of HRPSO with those of the HS and PSO is shown in Fig. 8.

5.2 A 72-bar spatial truss

A 72-bar spatial truss shown in Fig. 9. Tab. 5 lists the values and directions of the two load cases applied to the 72 bar spatial truss. It has been size optimized by many researchers [12, 14–16, 20, 23, 24]. In these studies, the material density and modulus of elasticity were 0.1 lb/in^3 (2767.990 kg/m^3) and 10,000 ksi (68950 MPa), respectively. The members were subjected to the stress limits of ± 25 ksi (± 172.375 MPa) and the uppermost nodes were subjected to the displacement limits of ± 0.25 in (± 0.635 cm) in both x and y direction. In this example, two cases are considered:

Case 1: in which the minimum cross-sectional area of all members is 0.1 in^2 (0.6452 cm^2) and Case 2: in which the minimum cross-sectional area of 0.01 in^2 (0.0645 cm^2) is considered. Tab. 6 shows the results for Case 1 and compares these results with those previously reported in the literature. In Case 1, the best weight of the HRPSO algorithm is 379.688 lb (1689 N). It gets the optimal solution after 153 iterations and 9180 function evaluations. The standard deviation of the HRPSO is 0.88 lb (3.91 N) which is better than those of the ACO, BB–BC and RO, being 3.66, 1.912 and 1.22 respectively. Tab. 7 shows the results for Case 2, In this case, HRPSO finds the best result while other algorithms could not reach an optimum design. Comparison between the allowable and existing stress and displacement constraint values of the HRPSO for Case 2 is shown in Fig. 10 and Fig. 11, it can be deduced that the second load condition is dominant. The convergence history for this example is shown in Fig. 12

5.3 A 120-bar dome truss

The topology and group members of a 120-bar dome truss are shown in **Fig. 13** This structure was first analyzed by Soh and Yang [25] to obtain the optimal sizing and configuration variables and then it was studied by Lee and Geem [15], Kaveh and Talatahari [8, 16] and Kaveh and Khayatazad [20]. In the example considered in these studies the size variables are considered to minimize the structural weight, so in this paper for better judgment the size optimizing is performed. The modulus of elasticity is 30,450 ksi (210000 MPa) and the material density is 0.288 lb/in^3 (7971.810 kg/m^3). The yield stress of steel is taken as 58.0 ksi (400 MPa). The dome is considered to be subjected to vertical loading at all the unsupported joints, these loads are taken as -13.49 kips (-60 kN) at node 1, -6.744 kips (-30 kN) at nodes 2 through 14, and -2.248 kips (-10 kN) at the rest of the nodes. The minimum cross-sectional area of all members is 0.775 in^2. (2 cm^2) The constraints are considered as:

(1) Stress constraints (according to the AISC ASD (1989))[26]

$$\begin{cases} \sigma_i^+ = 0.6F_y & for\ \sigma_i \geq 0 \\ \sigma_i^- & for\ \sigma_i < 0 \end{cases}$$

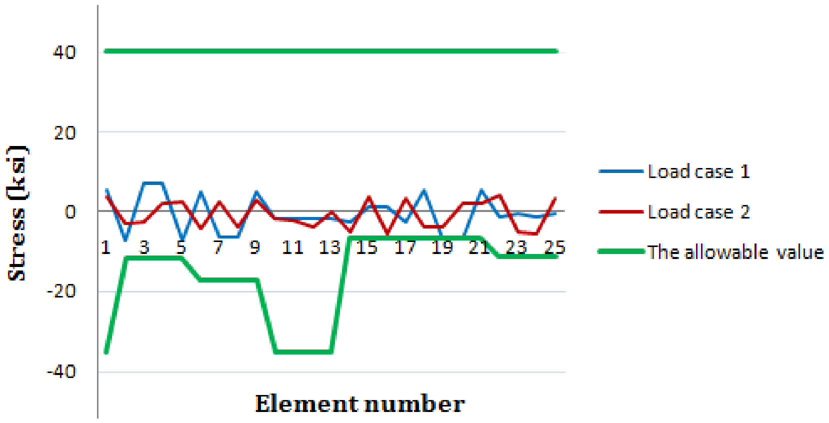

Fig. 6. Comparison of the allowable and existing stresses in the elements of the 25-bar space truss using HRPSO.

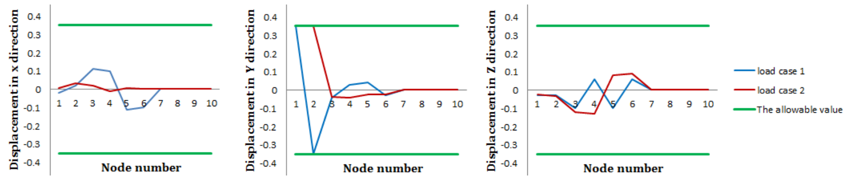

Fig. 7. Comparison of the allowable and existing displacements for the nodes of the 25-bar space truss using HRPSO.

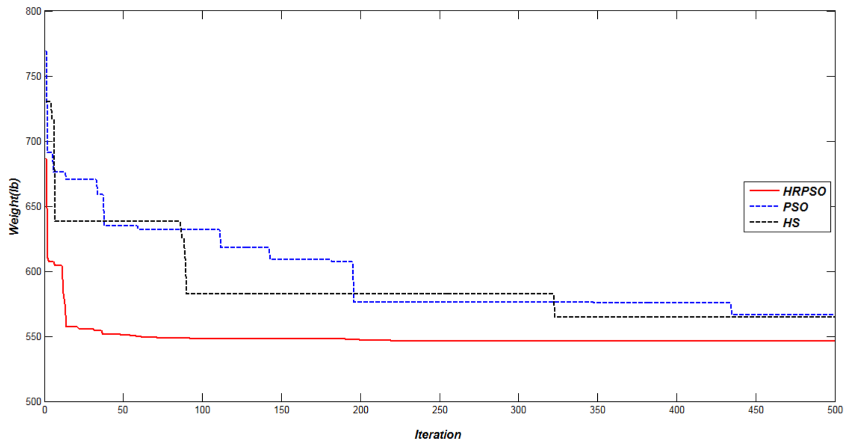

Fig. 8. Comparison of the convergence rates between the three algorithms for the 25-bar space truss structure.

Tab. 4. Optimal design comparison for the 25-bar space truss.

Element group		Optimal cross-sectional areas (in^2)										
		Rizzi [21]	Camp and Bichon [12]	Lee and Geem [15]	Li et al. [22]			Kaveh and Talatahari [8]	Camp [23]	Kaveh and Talatahari [16]	Present work	
			ACO	HS	PSO	PSOPC	HPSO	HPSACO	BB-BC	HBB-BC	in^2	cm^2
1	A1	0.010	0.010	0.047	9.863	0.010	0.010	0.010	0.010	0.010	0.010	0.0645
2	A2~A5	1.988	2.000	2.022	1.798	1.979	1.970	2.054	2.092	1.993	1.969	12.7032
3	A6~A9	2.991	2.966	2.950	3.654	3.011	3.016	3.008	2.964	3.056	3.016	19.4580
4	A10~A11	0.010	0.010	0.010	0.100	0.100	0.010	0.010	0.010	0.010	0.010	0.0645
5	A12~A13	0.010	0.012	0.014	0.100	0.100	0.010	0.010	0.010	0.010	0.010	0.0645
6	A14~A17	0.684	0.689	0.668	0.596	0.657	0.694	0.679	0.689	0.665	0.681	4.3935
7	A18~A21	1.677	1.679	1.657	1.659	1.678	1.681	1.611	1.601	1.642	1.681	10.8451
8	A22~A25	2.663	2.668	2.663	2.612	2.693	2.643	2.678	2.686	2.679	2.657	17.1419
Weight(lb)		545.16	545.53	544.38	627.08	545.27	545.19	544.99	545.38	545.16	544.99	2424.2 N

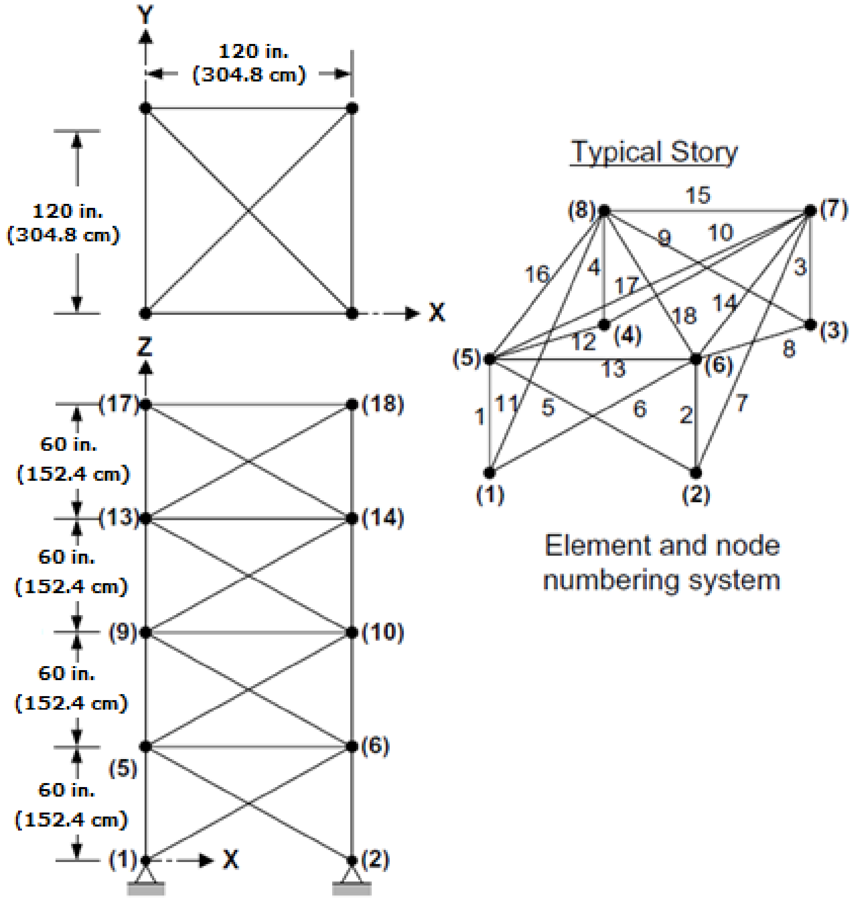

Fig. 9. A 72-bar spatial truss.

Tab. 5. Loading conditions for the 72-bar spatial truss.

Node	Case 1			Case 2		
	P_X kips (kN)	P_Y kips (kN)	P_Z kips (kN)	P_X kips (kN)	P_Y Kips (kN)	P_Z kips (kN)
17	5.0 (22.25)	5.0 (22.25)	-5.0 (22.25)	0.	0.	-5.0 (22.25)
18	0.0	0.0	0.0	0.0	0.0	-5.0 (22.25)
19	0.0	0.0	0.0	0.0	0.0	-5.0 (22.25)
20	0.0	0.0	0.0	0.0	0.0	-5.0 (22.25)

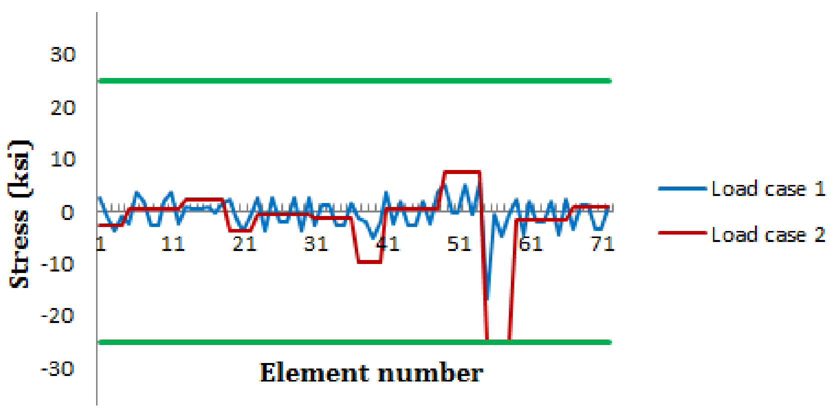

Fig. 10. Comparison of the allowable and existing stresses in the elements of the 72-bar space truss using HRPSO (Case 2).

Tab. 6. Optimal design comparison for the 72-bar space truss (Case 1).

Element group		Optimal cross-sectional areas (in^2)									
		Khan and Willmert [24]		Camp and Bichon [12]	Lee and Geem [15]	Perez and Behdinan [14]	Camp [23]	Kaveh and Talatahari [16]	Kaveh and Khayatazad [20]	Present work	
				ACO	HS	PSO	BB-BC	HBB-BC	RO	in^2	cm^2
		$\eta = 0.1$	$\eta = 0.15$								
1	A1~A4	1.793	1.859	1.948	1.790	1.7427	1.8577	1.9042	1.836490	1.83100	11.8129
2	A5~A12	0.522	0.526	0.508	0.521	0.5185	0.5059	0.5162	0.502096	0.50954	3.2873
3	A13~A16	0.100	0.100	0.101	0.100	0.1000	0.1000	0.1000	0.100007	0.10000	0.6452
4	A17~A18	0.100	0.100	0.102	0.100	0.1000	0.1000	0.1000	0.100390	0.10000	0.6452
5	A19~A22	1.208	1.253	1.303	1.229	1.3079	1.2476	1.2582	1.252233	1.26539	8.1638
6	A23~A30	0.521	0.524	0.511	0.522	0.5193	0.5269	0.5035	0.503347	0.50610	3.2652
7	A31~A34	0.100	0.100	0.101	0.100	0.1000	0.1000	0.1000	0.100176	0.10000	0.6452
8	A35~A36	0.100	0.100	0.100	0.100	0.1000	0.1012	0.1000	0.100151	0.10000	0.6452
9	A37~A40	0.623	0.581	0.561	0.517	0.5142	0.5209	0.5178	0.572989	0.51550	3.3258
10	A41~A48	0.523	0.527	0.492	0.504	0.5464	0.5172	0.5214	0.549872	0.53250	3.4355
11	A49~A52	0.100	0.100	0.100	0.100	0.1000	0.1004	0.1000	0.100445	0.10000	0.6452
12	A53~A54	0.196	0.158	0.107	0.101	0.1095	0.1005	0.1007	0.100102	0.10019	0.6464
13	A55~A58	0.149	0.152	0.156	0.156	0.1615	0.1565	0.1566	0.157583	0.15611	1.0072
14	A59~A66	0.570	0.561	0.550	0.547	0.5092	0.5507	0.5421	0.522220	0.55790	3.5993
15	A67~A70	0.443	0.438	0.390	0.442	0.4967	0.3922	0.4132	0.435582	0.41360	2.6684
16	A71~A72	0.519	0.532	0.592	0.590	0.5619	0.5922	0.5756	0.597158	0.55304	3.5680
Weight (lb)		381.72	387.67	380.24	379.27	381.91	379.85	379.66	380.458	379.688	1689 N

Tab. 7. Optimal design comparison for the 72-bar space truss (Case 2).

Element group		Optimal cross-sectional areas (in^2)		
		Lee and Geem [15]	Present work	
		HS	in^2	cm^2
1	A1~A4	1.963	1.88900	12.1871
2	A5~A12	0.481	0.53020	3.4206
3	A13~A16	0.010	0.01000	0.0645
4	A17~A18	0.011	0.01000	0.0645
5	A19~A22	1.233	1.31480	8.4826
6	A23~A30	0.506	0.50929	3.2857
7	A31~A34	0.011	0.01000	0.0645
8	A35~A36	0.012	0.01000	0.0645
9	A37~A40	0.538	0.52950	3.4161
10	A41~A48	0.533	0.52634	3.3957
11	A49~A52	0.010	0.01000	0.0645
12	A53~A54	0.167	0.08941	0.5768
13	A55~A58	0.161	0.16927	1.0921
14	A59~A66	0.542	0.52700	3.4000
15	A67~A70	0.478	0.42545	2.7448
16	A71~A72	0.551	0.59162	3.8169
Weight (lb)		364.33	363.943	1618.9 N

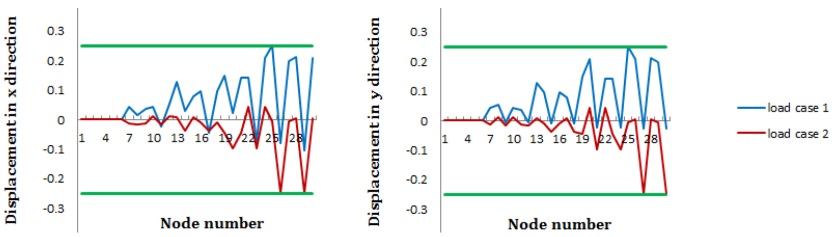

Fig. 11. Comparison of the allowable and existing displacements for the nodes of the 72-bar space truss using HRPSO (Case 2).

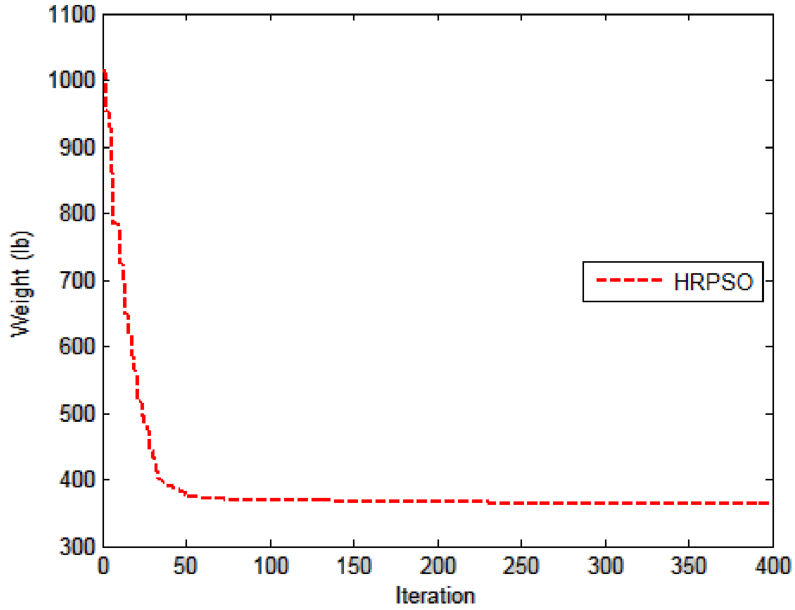

Fig. 12. Convergence rate for the 72-bar spatial truss structure using HRPSO (Case 2).

Where σ_i^- is calculated according to the slenderness ratio:

$$\sigma_i^- = \begin{cases} \left[\left(1-\frac{\lambda_i^2}{2C_C^2}\right)F_y\right] / \left(\frac{5}{3}+\frac{3\lambda_i}{8C_C}-\frac{\lambda_i^3}{8C_C^3}\right) & for \lambda_i < C_C \\ \frac{12\pi^2 E}{23\lambda_i^2} & for \lambda_i \geq C_C \end{cases}$$

Where E = the modulus of elasticity; F_y = the yield stress of steel; Cc = the slenderness ratio (λ_i) dividing the elastic and inelastic buckling regions $\left(C_C = \sqrt{2\pi^2 E/F_y}\right)$; λ_i the slenderness ratio ($\lambda_i = kL_i/r_i$); k = the effective length factor; L_i = the member length; and r_i = the radius of gyration. On the other hand, the radius of gyration (r_i) can be expressed in terms of cross-sectional areas, i.e., $r_i = aA_i^b$ [27] , Here, a and b are the constants depending on the types of sections adopted for the members such as pipes, angles, and tees. In this example, pipe sections (a = 0.4993 and b = 0.6777) were adopted for bars and four cases of constraints were considered:

Case 1: with stress constraints and no displacement constraints

Case 2: stress constraints and displacement limitations of ± 0.1969 in (± 5 mm) are imposed on all nodes in x- and y-directions.

Case 3: no stress constraints but displacement limitations of ± 0.1969 in (± 5 mm) imposed on all nodes in z-directions.

Case 4: all constraints explained above

Tab. 8 gives the best solution and the corresponding weights for all cases. HRPSO needs nearly 16000 function evaluations to reach a solution which is less than 35,000 and 19850 for HS [15] and RO [20] respectively. Fig. 14 to Fig. 19 compare the allowable and existing stress and displacement constraint values of the HRPSO resulted in four cases. By analyzing these charts, it can be inferred that in Case 1, the stress constraints of some elements in the 2nd, 4th and 7th groups are active. In Case 2, the stress constraints of some elements in the 2nd, 4th and 7th groups and the displacement of node 26 in y direction are active. The maximum value for displacement in the x direction is 0.1835 in (0.4661 cm) and the maximum displacement in the y direction is 0.1967 in (0.4996 cm). The active constraints for Case 3 are the displacements of the node 6 and node 10 in z directions which is 0.1969 in (0.5001 cm). In Case 4, the stresses in the elements of the 7th group and the displacements of the 2nd to 13th nodes in z directions affect the results.

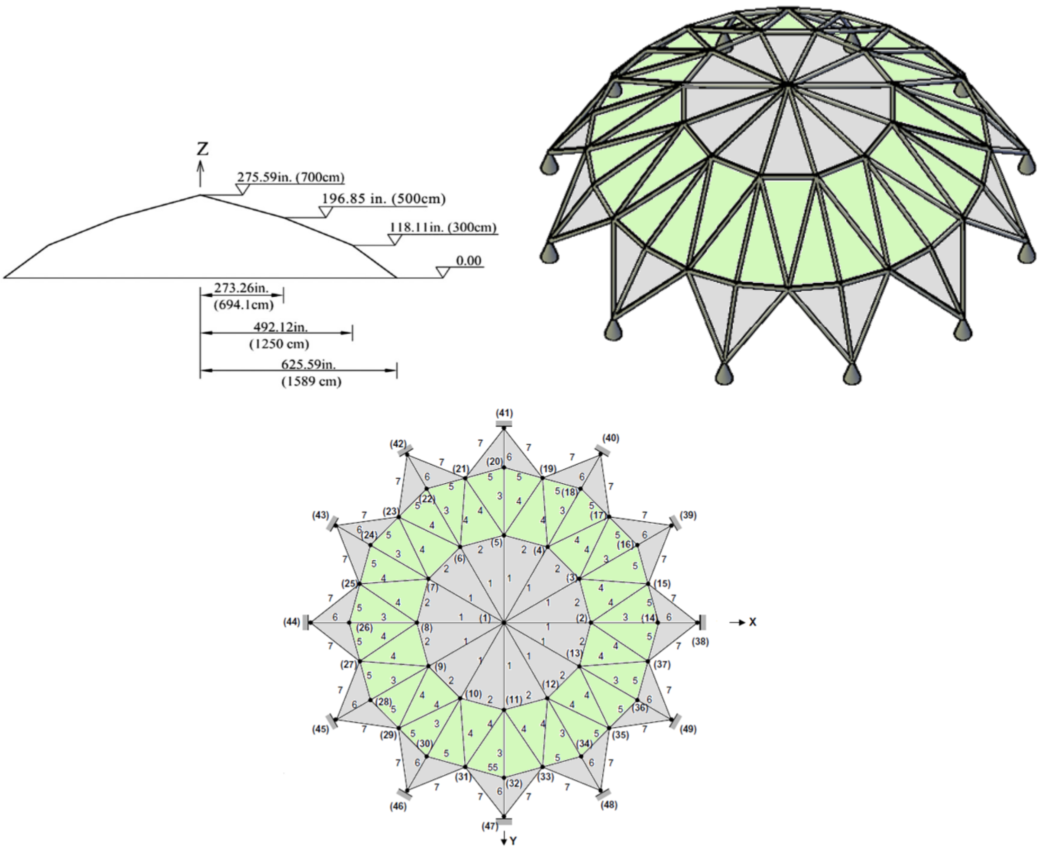

Fig. 13. A 120-bar dome truss.

Tab. 8. Optimal design comparison for the 120-bar dome truss (Case 1).

Element group		Optimal cross-sectional areas (in^2)						
		Lee and Geem [15]			Kaveh and Talatahari [8]	Kaveh and Khayatazad [20]	Present work	
		HS	PSO	PSOPC	HPSACO	RO	in^2	cm^2
1	A1	3.295	3.147	3.235	3.311	3.128	3.1215	20.138
2	A2	2.396	6.376	3.370	3.438	3.357	3.3547	21.643
3	A3	3.874	5.957	4.116	4.147	4.114	4.1136	26.539
4	A4	2.571	4.806	2.784	2.831	2.783	2.7808	17.941
5	A5	1.150	0.775	0.777	0.775	0.775	0.7750	5.000
6	A6	3.331	13.798	3.343	3.474	3.302	3.3014	21.299
7	A7	2.784	2.452	2.454	2.551	2.453	2.4448	15.773
Weight (lb)		19707.77	32432.9	19618.7	19491.3	19476.193	19451.59	86525 N

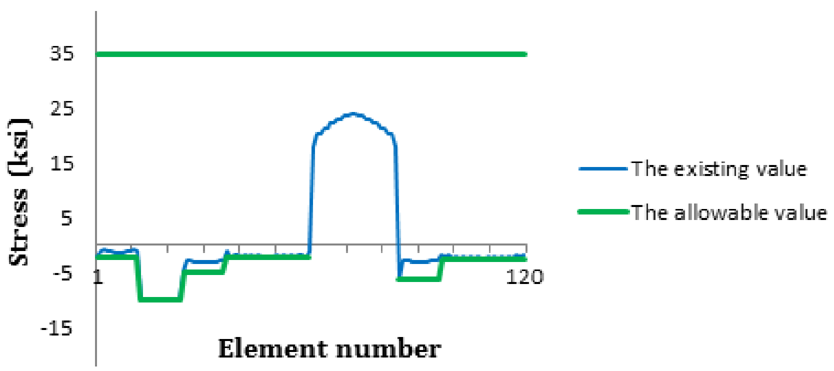

Fig. 14. Comparison of the allowable and existing stresses in the elements of the 120-bar dome truss using HRPSO (Case 1).

Tab. 9. Optimal design comparison for the 120-bar dome truss (Case 2).

Element group		Optimal cross-sectional areas (in^2)						
		Lee and Geem [15]			Kaveh and Talatahari [8]	Kaveh and Khayatazad [20]	Present work	
		HS	PSO	PSOPC	HPSACO	RO	in^2	cm^2
1	A1	3.296	15.97	3.083	3.779	3.084	3.0811	19.878
2	A2	2.789	9.599	3.639	3.377	3.360	3.3525	21.629
3	A3	3.872	7.467	4.095	4.125	4.093	4.0964	26.428
4	A4	2.570	2.790	2.765	2.734	2.762	2.7616	17.817
5	A5	1.149	4.324	1.776	1.609	1.593	1.5943	10.286
6	A6	3.331	3.294	3.779	3.533	3.294	3.2926	21.243
7	A7	2.781	2.479	2.438	2.539	2.434	2.4326	15.694
Weight (lb)		19893.34	41052.7	20681.7	20078.0	20071.9	20066.34	89259.5 N

Tab. 10. Optimal design comparison for the 120-bar dome truss (Case 3).

Element group		Optimal cross-sectional areas (in^2)						
		Keleşoğlu and Ülker [28]			Kaveh and Talatahari [8]	Kaveh and Khayatazad [20]	Present work	
			PSO	PSOPC	HPSACO	RO	in^2	cm^2
1	*A1*	*5.606*	*1.773*	*2.098*	*2.034*	*2.044*	*1.92122*	12.395
2	*A2*	*7.750*	*17.635*	*16.444*	*15.151*	*15.665*	*15.02707*	96.949
3	*A3*	*4.311*	*7.406*	*5.613*	*5.901*	*5.848*	*5.89393*	38.025
4	*A4*	*5.424*	*2.153*	*2.312*	*2.254*	*2.290*	*2.15754*	13.920
5	*A5*	*4.402*	*15.232*	*8.793*	*9.369*	*9.001*	*9.66101*	62.329
6	*A6*	*6.223*	*19.544*	*3.629*	*3.744*	*3.673*	*3.71555*	23.971
7	*A7*	*5.405*	*0.800*	*1.954*	*2.104*	*1.971*	*1.95459*	12.610
Weight (lb)		38237.83	46893.5	31776.2	31670.0	31733.2	31693.04	140977.6 N

Tab. 11. Optimal design comparison for the 120-bar dome truss (Case 4).

Element group		Optimal cross-sectional areas (in^2)					
				Kaveh and Talatahari [8]	Kaveh and Khayatazad [20]	Present work	
		PSO	PSOPC	HPSACO	RO	in^2	cm^2
1	A1	12.802	3.040	3.095	3.030	3.0231	19.504
2	A2	11.765	13.149	14.405	14.806	15.5518	100.334
3	A3	5.654	5.646	5.020	5.440	4.9536	31.959
4	A4	6.333	3.143	3.352	3.124	3.0958	19.973
5	A5	6.963	8.759	8.631	8.021	8.2583	53.279
6	A6	6.492	3.758	3.432	3.614	3.3255	21.455
7	A7	4.988	2.502	2.499	2.487	2.4958	16.102
Weight (lb)		51986.2	33481.2	33248.9	33317.8	33281.12	148041.8 N

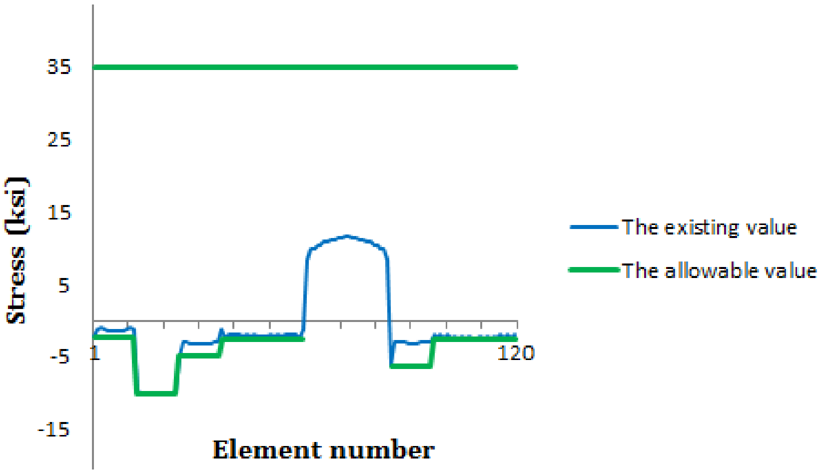

Fig. 15. Comparison of the allowable and existing stresses in the elements of the 120-bar dome truss using HRPSO (Case 2).

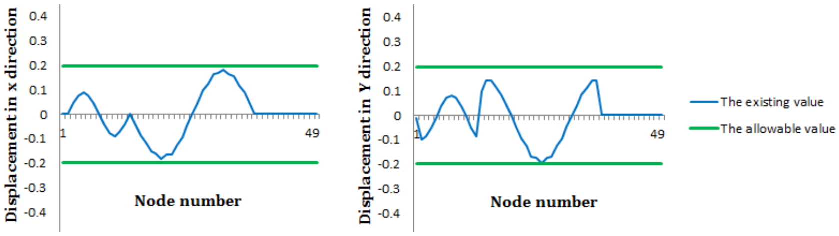

Fig. 16. Comparison of the allowable and existing displacements for the 120-bar dome truss using HRPSO (Case 2).

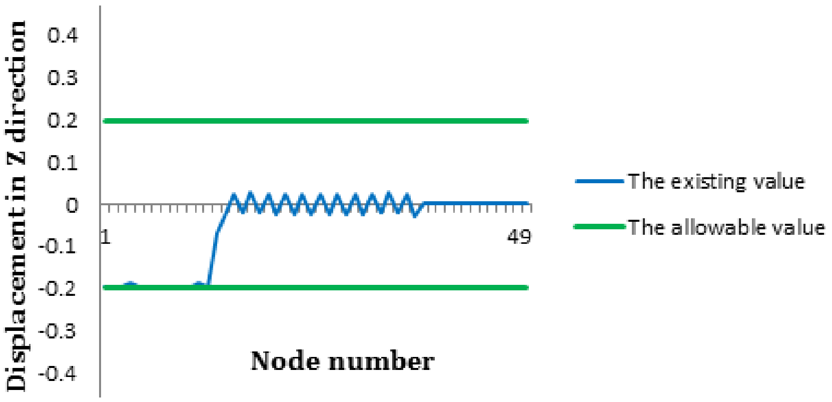

Fig. 17. Comparison of the allowable and existing displacements for the 120-bar dome truss using HRPSO (Case 3).

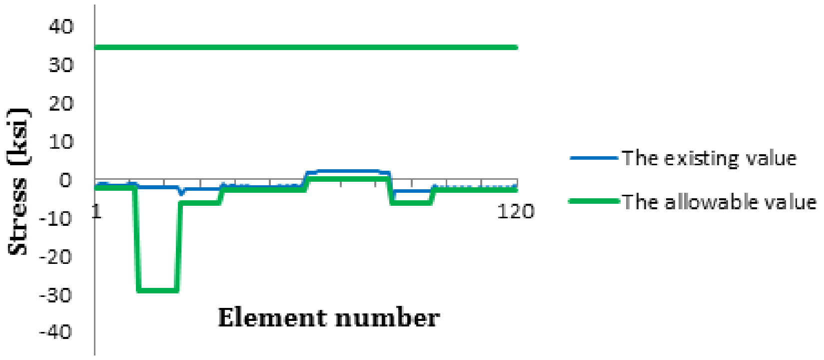

Fig. 18. Comparison of the allowable and existing stresses in the elements of the 120-bar dome truss using HRPSO (Case 4).

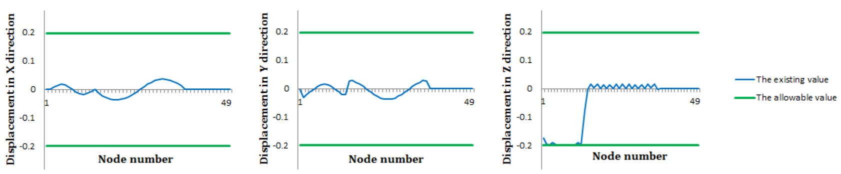

Fig. 19. Comparison of the allowable and existing displacements for the 120-bar dome truss using HRPSO (Case 4).

5.4 A 200-bar planar truss

Fig. 20 shows the 200-bar planar truss which all members are made of steel: the material density and modulus of elasticity are 0.283 lb/in^3 (7933.410 kg/m^3) and 30,000 ksi (206000 MPa), respectively. This truss is subjected to constraints only on stress limitations of ±10 ksi (68.95 MPa). The minimum admissible cross-sectional area is 0.1 in^2. (0.6452 cm^2) There are three loading conditions: (1) 1.0 kip (4.45 kN) acting in the positive x- direction at nodes 1, 6, 15, 20, 29, 43, 48, 57, 62, and 71; (2) 10 kips (44.5 kN) acting in the negative y-direction at nodes 1, 2, 3, 4, 5,6, 8, 10, 12, 14, 15,16, 17, 18, 19, 20, 22, 24,..., 71, 72, 73, 74 and 75; and (3) Conditions (1) and (2) acting together. The 200 members of this truss are divided into 29 groups, as shown in Tab. 12.

The HRPSO algorithm found the best weight as 25451.95 lb after 34000 function evaluations. A comparison to other references with respect to the cross-sectional area of each group and the final weight reached for the Two-hundred bar planar truss is shown in the Tab. 12. In some studies the allowable stresses have been considered as approximately 10.4 ksi (46.26 kN), In this case the HRPSO algorithm found the best weight as 24853.5 lb (110553.9 N) and the solution vector was: (0.1058, 0.8925 , 0.178 , 0.1049, 1.879, 0.3052, 0.1006, 2.9898, 0.2781, 3.9236, 0.4434, 0.103, 5.2836, 0.1566, 6.1959, 0.572, 0.1005, 7.8522, 0.1197 ,8.6529 ,0.6757 ,0.1519, 10.3116, 0.3816, 11.284 ,0.9516, 7.0692, 10.7735 ,13.0702).

6 CONCLUDING REMARKS

In this paper the recently developed metaheuristic population-based search “RO” is mixed with PSO and HS [29]. In HRPSO, the PSO acts as the main engine of the algorithm, and origin making in RO boosts the movement vector of the particles and improve the exploration On the other hand, the HS is used as an auxiliary tool for enhancing the local search and better exploitation Beyond these exploration and exploitation features, HRPSO decrease some parameters which are needed in PSO.

Four truss structures are considered to verify the efficiency of the HRPSO algorithm. In comparison to other metaheuristic algorithms, the HRPSO algorithm has better performance than ACO, PSO and even better than HS and RO (in some cases).

Acknowledgement

The first author is grateful to the Iran National Science Foundation for the support.

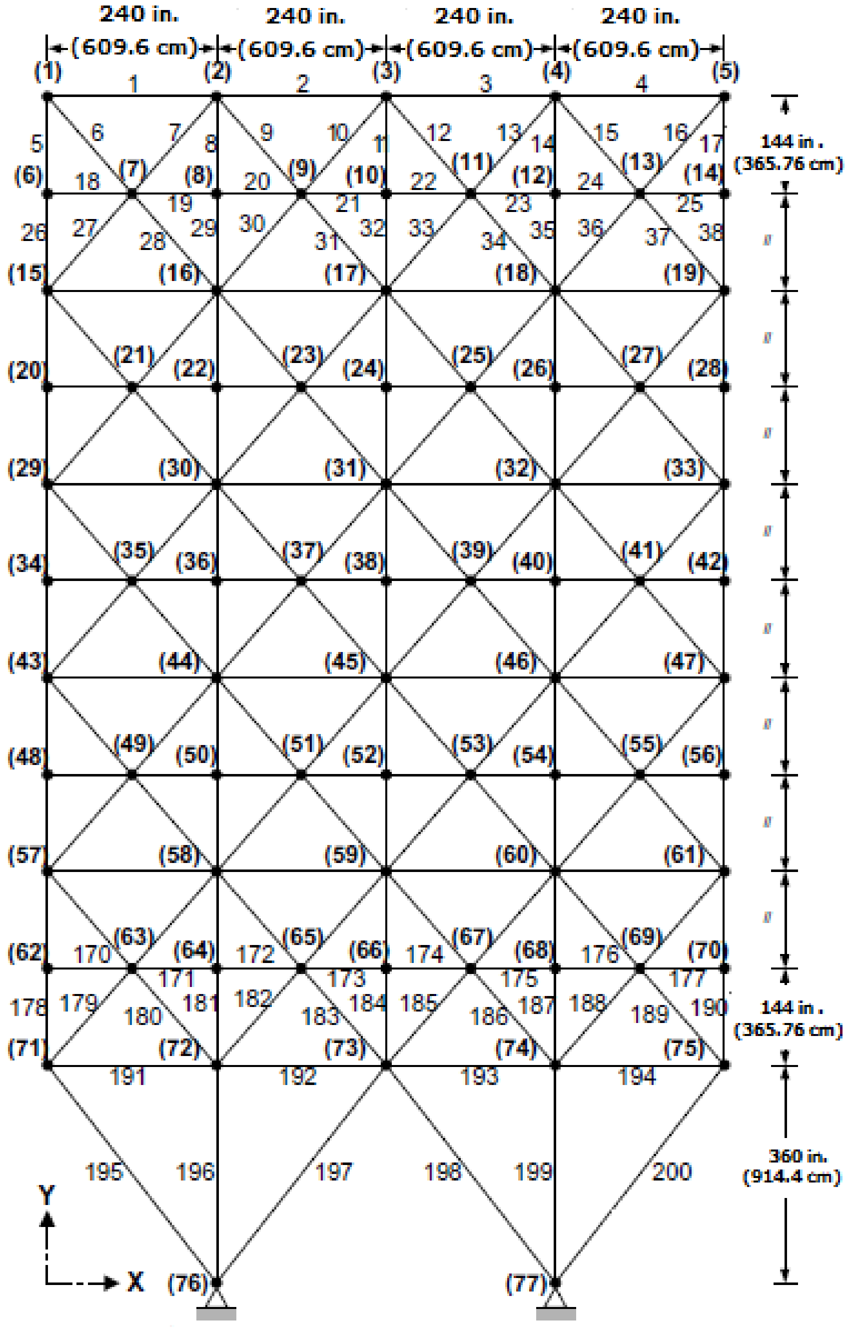

Fig. 20. A 200-bar planar truss.

Tab. 12. Optimal design comparison for the 200-bar planar truss

Group	Variables members (A_i, i = 1,...,200)	Optimal cross-sectional areas (in^2)			
		Lee and Geem [16]		Present work	
		HS	PSO	in^2	cm^2
1	1,2,3,4	0.1253	0.1038	0.1463	0.9439
2	5,8,11,14,17	1.0157	1.0763	0.9440	6.0903
3	19,20,21,22,23,24	0.1069	0.1000	0.1000	0.6452
4	18,25,56,63,94,101, 132,139,170,177	0.1096	0.1556	0.1000	0.6452
5	26,29,32,35,38	1.9369	1.9468	1.9399	12.515
6	6,7,9,10,12,13,15,16, 27,28,30,31,33,34,36, 37	0.2686	0.2656	0.2965	1.9129
7	39,40,41,42	0.1042	0.1299	0.1000	0.6452
8	43,46,49,52,55	2.9731	3.0653	3.1050	20.032
9	57,58,59,60,61,62	0.1309	0.1221	0.1000	0.6452
10	64,67,70,73,76	4.1831	4.0538	4.1052	26.485
11	44,45,47,48,50,51,53, 54,65,66,68,69,71,72, 74,75	0.3967	0.3764	0.4030	2.6000
12	77,78,79,80	0.4416	0.1111	0.1926	1.2426
13	81,84,87,90,93	5.1873	4.7229	5.4285	35.022
14	95,96,97,98,99,100	0.1912	13.8382	0.1000	0.6452
15	102,105,108,111,114	6.241	5.7394	6.4280	41.470
16	82,83,85,86,88,89,91, 92,103,104,106,107, 109,110,112,113	0.6994	1.4790	0.5733	3.6987
17	115,116,117,118	0.1158	0.1022	0.1378	0.8890
18	119,122,125,128,131	7.7643	8.1039	7.9731	51.439
19	133,134,135,136,137, 138,140,143,146,149, 152	0.1000	0.1000	0.1000	0.6452
20	140,143,146,149,152	8.8279	9.2087	8.9727	57.888
21	120,121,123,124,126, 127,129,130,141,142, 144,145,147,148,150, 151	0.6986	1.0012	0.7073	4.5632
22	153,154,155,156	1.5563	0.1146	0.4200	2.7097 N
23	157,160,163,166,169	10.9806	10.8325	10.867	70.111
24	171,172,173,174,175, 176	0.1317	8.3898	0.1000	0.6452
25	178,181,184,187,190	12.1492	11.9764	11.867	76.561
26	158,159,161,162,164, 165,167,168,179,180, 182,183,185,186,188, 189	1.6373	3.7262	1.0338	6.6697
27	191,192,193,194	5.0032	2.3484	6.6839	43.121
28	195,197,198,200	9.3545	8.2921	10.809	69.736
29	196,199	15.0919	17.0625	13.837	89.270
Weight (lb)		25447.1	31162.1	25451.95	113215.9 N

References

1 **Holland J**, *Adaptation in natural and artificial systems*, University of Michigan Press; Ann Arbor, 1975.

2 **Eberhart R, Kennedy J**, *A new optimizer using particle swarm theory*, In: Micro Machine and Human Science, Proceedings of the IEEE Sixth International Symposium, 1995, pp. 39–43.

3 **Kennedy J, Eberhart R**, *Particle swarm optimization*, In: Neural Networks, Proceedings of the IEEE International Conference, 1995, pp. 1942–1948.

4 **Dorigo M, Maniezzo V, Colorni A**, *Ant system: optimization by a colony of cooperating agents, Man, and Cybernetics*, In: Part B: Cybernetics, IEEE Transactions, 1996, pp. 29–41.

5 **Kaveh A, Talatahari S**, *A novel heuristic optimization method: charged system search*, Acta Mechanica, **213**(3-4), (2010), 267–289, DOI 10.1007/s00707-009-0270-4.

6 **Kaveh A, Khayatazad M**, *A new meta-heuristic method: Ray Optimization*, Computers and Structures, **112**, (2012), 283–294, DOI 10.1016/j.compstruc.2012.09.003.

7 **He S, Wu Q, Wen J, Saunders J, Paton R**, *A particle swarm optimizer with passive congregation*, Biosystems, **78**(1-3), (2004), 135–147, DOI 10.1016/j.biosystems.2004.08.003.

8 **Kaveh A, Talatahari S**, *Particle swarm optimizer, ant colony strategy and harmony search scheme hybridized for optimization of truss structures*, Computers and Structures, **87**(5-6), (2009), 267–283, DOI 10.1016/j.compstruc.2009.01.003.

9 **Csébfalvi A**, *A hybrid meta-heuristic method for continuous engineering optimization*, Periodica Polytechnica Civil Engineering, **53**(2), (2009), 93–100, DOI 10.3311/pp.ci.2009-2.05.

10 **Csébfalvi A**, *Multiple constrained sizing-shaping truss-optimization using ANGEL method*, Periodica Polytechnica Civil Engineering, **55**(1), (2011), 81–86, DOI 10.3311/pp.ci.2011-1.10.

11 **Toğan V, Daloğlu AT**, *Optimization of 3d trusses with adaptive approach in genetic algorithms*, Engineering Structures, **28**(7), (2006), 1019–1027, DOI 10.1016/j.engstruct.2005.11.007.

12 **Camp C, Bichon B**, *Design of space trusses using ant colony optimization*, Journal of Structural Engineering ASCE, **130**(5), (2004), 741–751, DOI 10.1061/(ASCE)0733-9445(2004)130:5(741).

13 **Schutte JF, Groenwold AA**, *Sizing design of truss structures using particle swarms*, Structural and Multidisciplinary Optimization, **25**(4), (2003), 261–269, DOI 10.1007/s00158-003-0316-5.

14 **Perez R, Behdinan K**, *Particle swarm approach for structural design optimization*, Computers and Structures, **85**(19-20), (2007), 1579–1588, DOI 10.1016/j.compstruc.2006.10.013.

15 **Lee K, Geem Z**, *A new structural optimization method based on the harmony search algorithm*, Computers and Structures, **82**(9-10), (2004), 781–798, DOI 10.1016/j.compstruc.2004.01.002.

16 **Kaveh A, Talatahari S**, *Size optimization of space trusses using Big Bang–Big Crunch algorithm*, Computers and Structures, **87**(17-18), (2009), 1129–1140, DOI 10.1016/j.compstruc.2009.04.011.

17 **Yang X**, *Engineering Optimization: An Introduction with Metaheuristic Applications*, John Wiley; UK, 2010, DOI 10.1002/9780470640425.

18 **Shi Y, Eberhart R**, *A modified particle swarm optimizer*, In:, pp. 69–73.

19 **Lee K, Geem Z**, *A new meta-heuristic algorithm for continuous engineering optimization: harmony search theory and practice*, Computer Method in Applied Mechanics and Engineering, **194**(36-38), (2005), 3902–3933, DOI 10.1016/j.cma.2004.09.007.

20 **Kaveh A, Khayatazad M**, *Ray optimization for size and shape optimization of truss structures*, Computers and Structures, **117**, (2013), 82–94, DOI 10.1016/j.compstruc.2012.12.010.

21 **Rizzi P**, *Optimization of multi-constrained structures based on optimality criteria*, In: Structures, Structural Dynamics, and Materials, Conference on AIAA/ASME/SAE 17th, 1976.

22 **Li L, Huang Z, Liu F, Wu Q**, *A heuristic particle swarm optimizer for optimization of pin connected structures*, Computers and Structures, **85**(7-8), (2007), 340–349, DOI 10.1016/j.compstruc.2006.11.020.

23 **Camp C**, *Design of space trusses using Big Bang–Big Crunch optimization*, Journal of Structural Engineering ASCE, **133**(7), (2007), 999–1008, DOI 10.1061/(ASCE)0733-9445(2007)133:7(999).

24 **Khan M, Willmert K, Thornton W**, *An Optimality Criterion Method for Large Scale Structures*, AIAA Journal, **17**(7), (1979), 753–761, DOI 10.2514/3.61214.

25 **Soh C, Yang J**, *Fuzzy Controlled Genetic Algorithm Search for Shape Optimization*, Journal of Computing in Civil Engineering, **10**(2), (1996), 143–150, DOI 10.1061/(ASCE)0887-3801(1996)10:2(143).

26 *Manual of Steel Construction-Allowable Stress Design*, American Institute of Steel Construction (AISC); Chicago, IL, 1989.

27 **Saka MP**, *Optimum Design of Pin-Jointed Steel Structures with Practical Applications*, Journal of Structural Engineering, **116**(10), (1990), 2599–2620, DOI 10.1061/(ASCE)0733-9445(1990)116:10(2599).

28 **Keleşoğlu O, Ülker M**, *Fuzzy optimization of geometrical nonlinear space truss design*, Turkish Journal of Engineering and Environmental Sciences, **29**, (2005), 321–329.

29 **Kaveh A**, *Advances in Metaheuristic Algorithms for Optimal Design of Structures*, Springer Verlag; Wien, 2010.